Early molecular imaging of interstitial changes in patients after myocardial infarction: Comparison with delayed contrast-enhanced magnetic resonance imaging

Johan Verjans, MD,[a] Sander Wolters, MD,[a] Ward Laufer, MD,[a] Mark Schellings, PhD,[a] Michelle Lax, MS,[c] Dagfinn Lovhaug, PhD,[d] Hendrikus Boersma, PharmD, PhD,[a] Gerrit Kemerink, PhD,[a] Simon Schalla, MD,[a] Paul Gordon, PhD,[c] Jaap Teule, MD, PhD,[a] Jagat Narula, MD, PhD,[a,b] and Leonard Hofstra, MD, PhD[a,b]

Introduction. **The clinical feasibility of noninvasive imaging of interstitial alterations after myocardial infarction (MI) was assessed using a technetium-99m-labeled RGD imaging peptide (RIP). In experimental studies, RIP has been shown to target integrins associated with collagen-producing myofibroblasts (MFB).**

Methods and Results. **Ten patients underwent myocardial perfusion imaging (MPI) within the first week after MI. At 3 and 8 weeks after MI, RIP was administered intravenously and SPECT images acquired for interstitial imaging. RIP imaging was compared to initial MPI and to the extent of scar formation defined by late gadolinium-enhanced (LGE) cardiac magnetic resonance (CMR) imaging 1 year after MI. RIP uptake was observed in 7 of the 10 patients at both 3 and 8 weeks. Although, RIP uptake corresponded to areas of perfusion defects, it usually extended beyond the infarct zone to a variable extent; 2 of 7 patients showed tracer uptake throughout myocardium. In all positive cases, RIP uptake was similar to the extent of scar observed at 1 year by LGE-CMR imaging.**

Conclusion. **This study demonstrates that RGD-based imaging early after MI may predict the eventual extent of scar formation, which often exceeds initial MPI deficit but colocalizes with LGE in CMR imaging performed subsequently. (J Nucl Cardiol 2010;17:1065–72.)**

Key Words: Molecular imaging • SPECT • infarction • myocardial • heart failure

INTRODUCTION

The process of ventricular remodeling after acute myocardial infarction (MI) plays an important role in predisposition to heart failure (HF).[1] Current morphology-based imaging modalities, such as cardiovascular magnetic resonance (CMR) imaging and echocardiography, provide excellent information about left ventricular (LV) chamber enlargement and dysfunction after MI.[2,3] However, these changes represent delayed and only partially reversible consequences of remodeling.[4,5] As such, clinical recognition of changes preceding clinically manifest ventricular remodeling may be of paramount importance for prevention of HF.[6,7] Remodeling is histopathologically characterized in addition to myocardial hypertrophy, by replacement and interstitial fibrosis, and may constitute worthy target

From the Cardiovascular Research Institute Maastricht,[a] Maastricht University Medical Center, Maastricht, The Netherlands; University of California, Irvine,[b] Irvine, CA; GE Healthcare,[c] Amersham, United Kingdom; and GE Healthcare,[d] Oslo, Norway.

We would like to dedicate this manuscript to Dagfinn Lovhaug, who passed away unexpectedly in July 2009, without whom this research would not have been possible.

This research was supported by the Dutch Heart Foundation NHS 2007B209.

Received for publication Jun 13, 2010; final revision accepted Jun 15, 2010.

Reprint requests: Jagat Narula, MD, PhD, University of California, Irvine, Irvine, CA; *narula@uci.edu*. Leonard Hofstra, Cardiovascular Research Institute Maastricht, Maastricht University Medical Center, P. Debyelaan 25, 6229 HX Maastricht, The Netherlands; *l.hofstra@ cardio.unimaas.nl*.

1071-3581/$34.00

doi:10.1007/s12350-010-9268-5

for identification of patients at high risk of developing HF and allow appropriate intervention.[8] Several candidate biological processes have been targeted for molecular imaging of cardiac remodeling.[9] The upregulation of the myocardial renin-angiotensin axis (RAS) has been proposed as potential target for identification of the likelihood of myocardial fibrosis.[10] Radiolabeled benzoyl lisinopril and losartan have been employed in pre-clinical studies for the noninvasive detection of intracellular angiotensin-converting enzyme and cell-membrane angiotensin II type 1 receptors, respectively, with the premise that characterization of subcellular changes should precede morphological evidence of remodeling.[11,12]

It has also been recently demonstrated that an RGD imaging peptide (RIP) successfully targeted proliferating myofibroblasts (MFB) in an experimental model of post-MI heart failure.[13] Although RIP-like molecules have been traditionally employed to target αvβ3 integrin expression associated with neoangiogenesis in tumors,[14,15] the experimental studies have revealed its localization in α-smooth muscle actin bearing MFB in the healing myocardium in >2-week-old MI. In experimental studies, RIP uptake maximizes at 2-4 weeks post-MI, and reduces substantially by 12 weeks. Use of antagonists of the RAS axis including ACE-inhibitors and angiotensin receptor blockers reduce the RIP uptake in post-MI animals, particularly in the remote myocardial regions. RIP uptake in these studies correlated with the extent of MFB infiltration and the magnitude of new collagen fiber deposition; tracer uptake also correlated with echocardiographic parameters of ventricular remodeling.[13,16]

In the present proof of concept study to explore clinical applicability of RIP, we employed a serial, 3- and 8-week imaging study with ^{99m}Tc-labeled RIP in patients following their first MI. The 3-week time point was chosen based on the abovementioned animal studies, which demonstrated a peak in tracer uptake between 2-4 weeks and a reduction by 6-12 weeks. The 8-week time point was chosen to see whether a similar pattern could be seen in patients. Subsequently, we compared RIP uptake to the infarct size by pre-discharge myocardial perfusion imaging and to the extent of fibrosis verified by late gadolinium-enhanced (LGE) CMR imaging 1-year later. Echocardiographic parameters of ventricular remodeling were obtained at baseline and serially during follow up.

METHODS

Twelve consecutive patients presenting with their first acute MI were prospectively enrolled between October 2005 and January 2006. No patient had a known history of coronary disease. All underwent coronary angiography and percutaneous coronary intervention (PCI) upon arrival in hospital. All patients were 18 years or older, and either male or post-menopausal/surgically sterile/nonpregnant females. Patients participating in other investigational drug studies within 30 days before this study or scheduled for one during follow-up of this study were excluded. Patients were also excluded if they were scheduled for a coronary artery bypass surgery within 30 days of study entry. The study complies with the Declaration of Helsinki and was approved by the institutional review board of the Maastricht University and Hospital. All patients provided informed consent in writing before enrollment.

A complete set of study data was available in 10 patients: entry, 3 and 8 weeks, and 6 and 12 months follow-up (Figure 1). Two patients were excluded before imaging: one due to a major gastric bleed and the other to coronary bypass surgery. At all time points, blood was collected for laboratory investigations, including pro-BNP, and antibodies against RIP (to exclude evidence of a possible immune response). Echocardiography was performed (iE33 ultrasound system, Philips Medical Systems, Andover, Massachusetts) at all follow-up

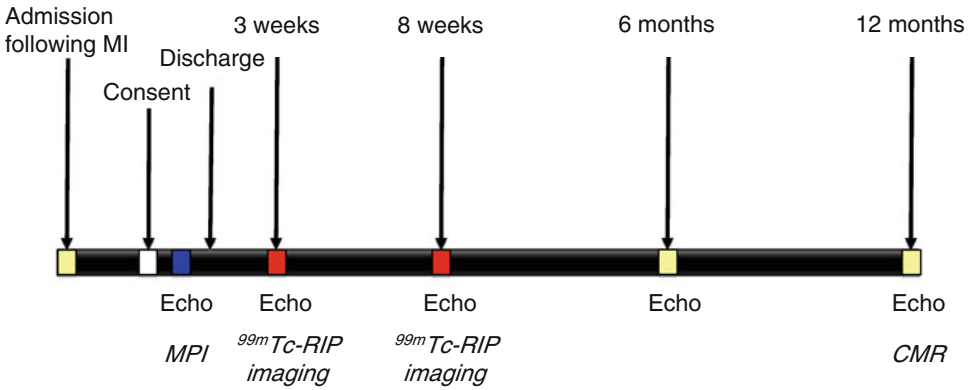

Figure 1. Schematic presentation of the clinical study protocol. Patients were enrolled during hospitalization for their first MI. All underwent myocardial perfusion imaging (MPI) before discharge from hospital. All patients were brought back for ^{99m}Tc-RIP scintigraphy at 3 and 8 weeks after MI. Echocardiography was performed at baseline, 3 and 8 weeks, and 6 and 12 months.

time-points. LV volumes and ejection fraction were obtained in the apical 4- and parasternal 2-chamber views. Nomenclature of LV segments and measurements of LV dimensions are based on the recommendations of the American Society of Echocardiography.[17] All patients were on aspirin, anti-platelet agents (aspirin and clopidogrel), statins, beta blockers and either ACE-inhibitor or ARB. Patients #1 and #9 also received a selective aldosterone receptor antagonist.

Myocardial Perfusion Imaging

Just before discharge from the hospital, all patients underwent (stress-rest) myocardial perfusion imaging (MPI) using a technetium-99m Sestamibi SPECT to define the extent of MI. For stress and rest MPI, 280 and 550 MBq (7.6 and 14.9 mCi) of MIBI was administered, respectively, and imaging was performed 1 hour later. The SPECT studies were performed with a triple-head gamma camera (Siemens Multi-SPECT-3, Hoffman Estates, IL, USA) as previously described.[18] The effective radiation dose was 2.2 mSv from the stress, and 4.5 mSv from the rest MPI.

^{99m}Technetium-RIP Imaging

RIP, a bi-cyclic peptide with an RGD motif, NC100692, was kindly supplied by GE Healthcare (Oslo, Norway). RIP SPECT imaging studies were performed at 1 and 2 hours after intravenous radiotracer administration, 3 and 8 weeks after MI; patients received not less than 780 MBq and not more than 949 MBq of radioactivity. The effective radiation dose from ^{99m}Tc-RIP is .008 mSv/MBq or a total of 7.8 mSv for a single injection of 1 GBq.

LGE-CMR Imaging

All patients underwent CMR imaging 12 ± 1.4 months after MI, using a 1.5T scanner (Intera, Philips Medical Systems, Best, the Netherlands). ECG-gated cine imaging was performed for evaluation of wall motion abnormalities, LV volumes, ejection fraction and mass, using a multi-phase, steady-state free precession sequence (bFFE). Continuous short axis images as well as single slices in 2- and 4-chamber and LV outflow tract view were obtained (TE 1.9 ms, TR 3.8 ms, flip angle 50°, slice thickness 6 mm, FOV 35 mm, scan matrix 256 × 256). LGE images were acquired approximately 10 minutes after injection of .2 mmol/kg Gd-DTPA, for infarct localization and infarct sizing, using a 3D T1-weighted inversion-recovery gradient-echo technique (continuous short axis, 2- and 4-chamber views, TE 1.3 ms, TR 4.2 ms, slice thickness 10 mm, flip angle 15°).

Image Analysis

Reconstruction and image display of all ^{99m}Tc-RIP scans were performed for all subjects, using a GE Healthcare Xeleris workstation V1.3, by one investigator, to ensure consistency. Filtered back-projection was then performed with a Hann pre-filter (cut-off frequency of .56 cycles per pixel, order 5.0), a reconstruction ramp filter, and a Butterworth post-filter (cut-off frequency of .52 cycles per pixel, order 5.0). No scatter or attenuation corrections were applied, but automatic motion correction was used when excessive movement was observed. Images were displayed in the CEqual color scale, in short, vertical, and horizontal axes slice orientations, as well as in polar plots with the 17-segment model overlay. The SPECT and SPECT/CMR image overlay was performed using the biomedical image quantification and kinetic modeling software package PMOD (PMOD Technologies LTD, Adliswil, Switzerland). Superimposition of combined MPI, 3- and 8-week RIP imaging was performed with automatic co-registration and alignment of reconstructed images; CMR images were superimposed by applying an additional scale correction necessitated by different resolutions of SPECT and CMR modalities.

Quantification of the area of uptake and total counts (normalized for injected activity) was recorded and change in radiotracer uptake in myocardium from 3 to 8 weeks was calculated (see Table 2). We used a descriptive semi-quantitative SPECT scoring for uptake (localization). Absolute counts were used in the evaluation of change of uptake between 3 and 8 weeks and defined as increased, no change, or decreased (+, = , −). The scoring could reliably be performed for the anterior wall infarctions and suboptimally in inferior infarctions, due to scattered hepatic uptake towards the inferior wall of the heart. Absolute counts from myocardial SPECT images could not be performed in the absence of attenuation correction.

CMR images were analyzed using CASS software (Piemedical Inc, Maastricht, the Netherlands). End-diastolic and end-systolic volumes were measured by manual delineation of endocardial and epicardial borders on continuous cine short axis images. Wall motion was analyzed visually and graded as normal, hypokinetic, akinetic, or dyskinetic. Localization, transmurality and size of infarct (%LV) were determined on late enhancement images with manual delineation of endocardial and epicardial as well as infarct borders.

RESULTS

Serial RIP Imaging After MI

Clinical characteristics of all patients are provided in Table 1. Of the 10 patients, 7 demonstrated myocardial RIP uptake both at 3 and 8 weeks; 3 patients showed no uptake (Figure 2). The difference in RIP uptake could reliably be calculated in 5 of 7 cases; total area of uptake increased in 2 patients at 8 weeks, and remained unchanged in the remaining 3 (see Table 2). There was a decrease in *total counts* in the region of interest in 2 patients, while the *area* of uptake area remained unchanged. There was an increase in the *total count* in region of interest in 3 of 5 patients, while the *area* of uptake increased in only 2 and remained unchanged in one. Technically, 2-hour post-injection

Table 1. Clinical characteristics

No.	Sex	Age	BMI	Symptoms	Artery	Intervention
1	F	39	26.8	VF	RCA prox	Primary PCI
2	F	49	25.9	AP	LAD D1	Primary PCI
3	M	72	23.8	AP	LAD mid	Primary PCI
4	M	55	22.8	VF	LAD prox	Primary PCI
5	F	63	27.5	AP	LAD prox	Primary PCI
6	M	59	32.7	AP	LAD prox + mid	Primary PCI
7	F	51	21.9	AP	RCA marg	Primary PCI
8	M	43	30.0	AP	RCA mid	Primary PCI
9	M	58	26	AP	Cx prox	Primary PCI + Thrombolysis
10	M	44	28	AP	RCA mid	Primary PCI

All culprit vessels demonstrated 99-100% occlusion except patient #6 (70-90%).
BMI, Body mass index; *VF*, ventricular fibrillation; *AP*, angina pectoris; *prox*, proximal; *marg*, marginal; *PCI*, percutaneous coronary intervention.

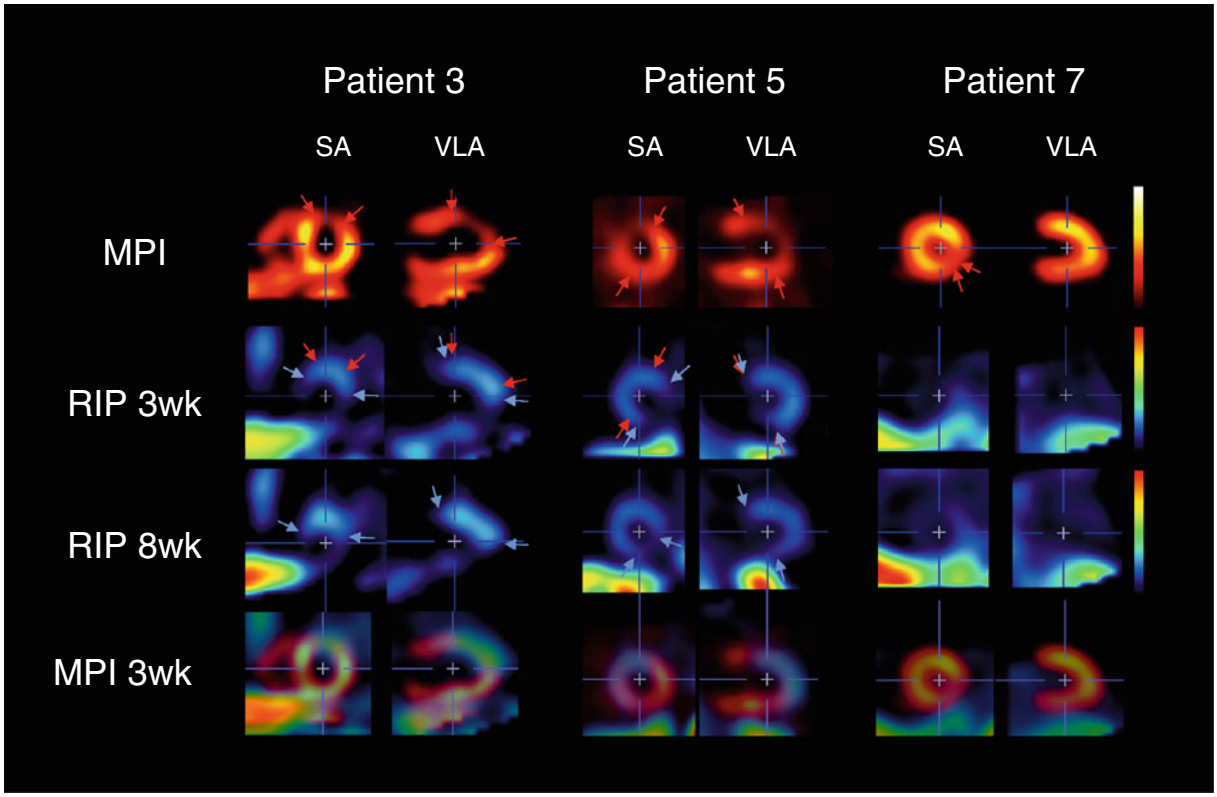

Figure 2. Stress MPI at discharge and ^{99m}Tc-RIP imaging at 3 and 8 weeks post-MI in 3 patients. The *left upper panel* demonstrates the short axis (SA) and vertical long axis (VLA) views of perfusion defects delineated by myocardial perfusion imaging (MPI) in the anterolateral region in patient #3 (*red arrows*). ^{99m}Tc-RIP images at 3 and 8 weeks (rows 2 and 3) show uptake (*blue arrows*) corresponding to the infarct and border zone delineated by MPI (*red arrows*). *L* denotes liver. The middle column shows patient #5 with a LAD region perfusion defect in MPI. ^{99m}Tc-RIP uptake in SA view extends beyond the infarct border zone at 3 and 8 weeks (*red* vs *blue arrows*). Patient #7 (*right panel*) is an example of a small RCA infarct (*red arrows*) with little or no ^{99m}Tc-RIP uptake at 3 and 8 weeks. The last row in all the panels represents fusion images of 3-week ^{99m}Tc-RIP and baseline MPI.

scans constituted similar but better image quality than those at 1 hour with higher target-to-background ratios.

Myocardial Perfusion Defects and RIP Uptake

As expected, myocardial perfusion defects correlated with the angiographic coronary artery involvement and echocardiographic wall motion abnormality. RIP uptake corresponded to the perfusion defects in all 7 patients with positive scans (Figure 2). In 5 of these 7 cases, uptake extended beyond the myocardial perfusion defect. In patients #4 and #5, RIP uptake extended from the infarct zone into the remote zone, and showed almost global uptake (Table 2).

RIP Uptake and CMR Imaging

The final extent of the scar tissue, as verified by LGE-CMR imaging, was established 1 year after MI. Mean LV mass was 103 ± 23 g and the infarct zone occupied 19.1 ± 11.6% of the myocardial area. RIP uptake at 3 and 8 weeks colocalized well in patients with the CMR-verified myocardial scar tissue (Figure 3). One patient with a large antero-apical and small septal scar by CMR showed colocalization with RIP uptake in both scar regions (Figure 3).

Evolution of LV Function Over 1 Year Follow-Up

During follow-up, mean LV ejection fraction decreased from 51 ± 10% at baseline to 47 ± 8% over time. LV ejection fraction decreased in 1 year by more than 10% in 2 patients. Patient #9 suffered from severe mitral valve regurgitation in a left circumflex coronary artery infarct and ejection fraction decreased from 59% to 39%. Patient #2 exhibited physical findings of HF including dyspnea and progressive shortness of breath during exercise; LV ejection fraction decreased from 47% to 37%. Pro-BNP decreased in all (except patient #7) from 95 ± 86 pmol/l at baseline to almost normal levels 25 ± 14 pmol/l at 12 months (see Table 2). No antibodies to RIP were detected in any of the patients.

DISCUSSION

Molecular imaging of MFB proliferation, employing Cy5.5-RIP, has recently been demonstrated as an indicator of new collagen deposition and myocardial remodeling in a post-MI mouse model.[13] This study shows the feasibility of clinical imaging with radiolabeled RIP in post-MI patients. Radiotracer uptake was observed in 7 of 10 patients and was predominantly localized within the infarct and peri-infarct region, but extended into the remote zones in two cases. Quantification of ^{99m}Tc-RIP in 5 positive patients at the 3- and 8-week intervals revealed increased extent of uptake in the myocardium at 8 weeks for 2 patients, whereas the remaining 3 patients showed no change in uptake at 8-weeks when compared to 3-week scans. Intriguingly, the extent of tracer uptake measured at 3 weeks co-localized with fibrotic regions delineated by CMR imaging at 1 year after MI, suggesting that the region visualized by RIP imaging might predict final scar formation after MI.

Following cardiomyocyte necrosis and the inflammatory process, proliferating myofibroblast and endothelial cell precursors migrate into the infarct zone replacing dead tissue with granulation tissue.[19] Concomitantly, αvβ3 integrins are upregulated in the infarct region.[20] It is well recognized that the expression of the β3 integrins contributes to angiogenesis in the peri-infarct zone as a part of the remodeling process, and occurs early, peaking about 7 days after MI. In a later stage, the αvβ3 integrins are associated with fibroblast-like cells, such as myofibroblast-producing collagens.[13,21] Over time, collagen fibrils are cross-linked by transglutaminase activity and myofibroblasts recede, resulting in a decrease in the integrin availability. Previous animal work from our lab suggests that uptake of our compound Cy5.5-labeled-RIP after MI period predominantly identifies the prevalence of myofibroblasts in the infarct region.[13] The observation that RIP uptake at 3 weeks co-localized well with the eventual extent of fibrosis verified by CMR, suggests that uptake by interstitial cells precedes localization of the scar subsequently. Some uptake of the tracer within the regions of angiogenesis (as observed after MI, hindlimb ischemia and in cancer employing similar integrin-targeting tracers) cannot be discounted,[14,15,22,23] we have not observed much angiogenesis in the transmurally scarred regions in our animal model at least 2 weeks after MI. Both the observations in the preclinical and the clinical studies using RIP indicate that uptake of the tracer is linked to eventual development of myocardial scar.

The number of patients included in this pilot study, and the variation in extent, density, and localization of remodeling parameters in the individual patient, makes it difficult to predict whether RIP imaging would help identify patients likely to develop LV remodeling. However, RIP imaging could hypothetically play a role in personalization of clinical management after MI. The neurohumoral antagonists are effective in the prevention of myocardial remodeling and use of them in combination has resulted in more favorable outcomes.[24,25] Various follow-up studies have demonstrated that many patients may not receive optimal therapy for various reasons, and identification of patients needing aggressive

Table 2. Angiographic profile, MPI, RIP imaging, ejection fraction, pro-BNP levels, and CMR parameters at baseline and follow-up

		MPI	^{99m}Tc-RIP uptake					LVEF (%)		Pro-BNP (pmol/l)		CMR	
No.	Coronary	Defect	Area 3 weeks	Area 8 weeks	ΔArea 3-8 weeks	ΔTC 3-8 weeks	Remote region	Baseline	ΔEF 0-12 M	Baseline	Δpro-BNP 0-12 *M*	LV mass (g)	Infarct size (%LV)
1	RCA prox	Large inferior wall	No uptake	No uptake	n/a	n/a	−	47	0	171	−145	76	21
2	LAD D1	Anterior and lateral-apical wall defects	Uptake antero-apical	Uptake antero-apical	=	−	−	47	−10	110	−84	83	26
3	LAD mid	Anterior-apical wall defect	Uptake antero-apical	Uptake antero-apical	+	+	−	48	1	174	−126	103	19
4	LAD prox	Large anterio-apical and inferior wall defects	Uptake antero-apical and inferior walls	Uptake antero-apical and inferior walls; remote uptake	+	+	+	33	7	200	−155	109	30
5	LAD prox	Large septal and anterio-apical wall defects	Focal areas of uptake corresponding to peri-infarct regions	Focal areas of uptake corresponding to peri-infarct regions; remote uptake	=	−	+	51	−3	215	−189	89	36
6	LAD prox + mid	Inferior wall and anterio-septal wall defects	Focal uptake in the anterior wall and apex	Focal uptake in the anterior wall and apex	=	+	−	51	2	41	−37	126	1
7	RCA marg	Basal-lateral and basal-inferior wall defects	No uptake	No uptake	n/a	n/a	−	66	−3	11	+1	68	9
8	RCA mid	Large inferior defect	Little focal uptake	Little focal uptake	n/a	n/a	−	45	−4	110	−82	134	16
9	Cx	Large inferior wall defect	Little focal uptake	Little focal uptake	n/a	n/a	−	59	−20	172	−148	113	27
10	RCA	Small inferior and anterior wall defects	No uptake	No uptake	n/a	n/a	−	56	3	31	−18	130	7

No, Number; *coronary*, coronary artery involved; *MPI*, myocardial perfusion imaging; *area*, area of uptake; Δ*TC*, Δtotal counts; *LV*, left ventricular; *EF* ejection fraction; *CMR*, cardiovascular magnetic resonance (infarct size by delayed enhancement).

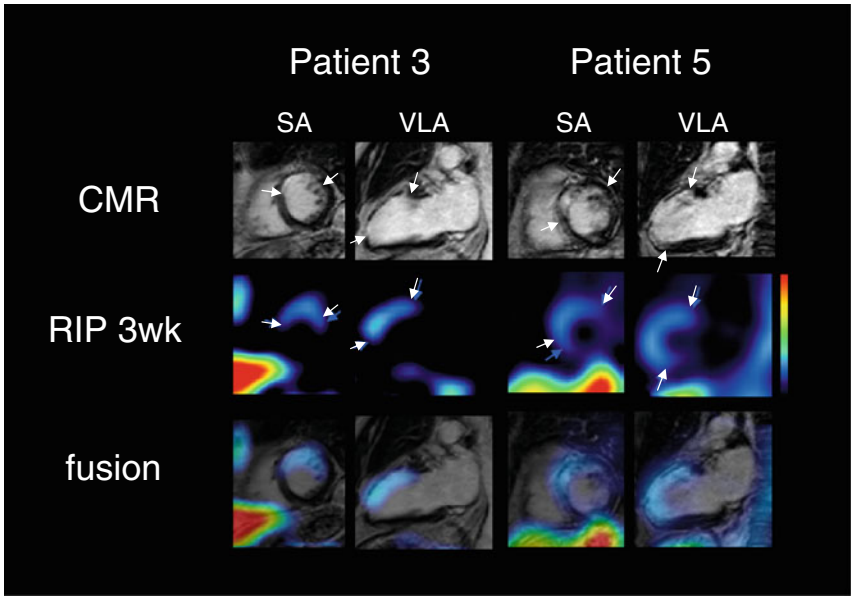

Figure 3. Co-localization of 3-week ^{99m}Tc-RIP uptake with CMR-verified evidence of fibrosis at 1 year. The first row demonstrates a CMR image of scar tissue in the LAD region (*white arrows*) in SA and VLA views for patients #3 and #5. The second row shows SA and VLA slices with ^{99m}Tc-RIP uptake (*blue arrows*) at 3 weeks after MI, corresponding to scar formation as determined by CMR after 1 year (*blue* vs *white arrows*). The last row shows SPECT/MR fusion images.

treatment may be of value as it reflects an earlier phase in the cascade of remodeling. It is also possible that serial interrogation with such imaging may facilitate optimization. We have recently reported the value of treatment with neurohumoral antagonists with Cy5.5-RIP uptake in an animal study, its correlation with remodeling parameters and the extent of myofibroblastic proliferation and collagen deposition.[13] We have initiated a larger clinical study to explore the capability of RIP imaging to evaluate efficacy of anti-fibrotic agents in post-infarct subjects.

The data presented here should be interpreted with caution due to a small number of patients. Nonetheless, the study offers a successful attempt of feasibility of molecular imaging for the evaluation of interstitial changes after MI in a clinical setting. Further, discrimination of tracer uptake in the inferior myocardial wall from liver uptake is a common limitation of SPECT nuclear imaging studies, and SPECT data are not fully quantitative. Finally, merging images at such distant time points might not be fully accurate. These limitations could significantly be mitigated by concomitant morphologic imaging, a strategy planned for our future study.

This study demonstrates proof of principle for imaging integrin upregulation in the infarct region in patients at early time points after MI. Since experimental data suggest that integrin upregulation is associated with fibroblastic activity (and hence with collagen deposition) the extent of radiolabeled RIP uptake may predict cardiac remodeling. The tracer uptake in this study colocalized with the LGE-CMR-verified myocardial fibrosis. Although we have focused on tracer uptake in the infarct region and surrounding myocardium, it will be necessary for clinical benefit that such an agent is able to pick up subtle increases in myofibroblastic activity in remote myocardium.

Disclosures

DL, ML, and PG are employees of GE Healthcare.

Open Access

References

1. Jessup M, Brozena S. Heart failure. N Engl J Med 2003;348:2007-18.
2. Sutton MS. Quantitative echocardiography in left ventricular remodeling after myocardial infarction. Curr Opin Cardiol 1996;11:378-85.

3. Lima JA, Desai MY. Cardiovascular magnetic resonance imaging: Current and emerging applications. J Am Coll Cardiol 2004;44:1164-71.
4. Corday E, Hajduczki I, O'Byrne GT, Kar S, Areeda J, Corday SR. Echocardiographic criteria to distinguish reversible from irreversible myocardial ischaemia. Eur Heart J 1988;9:29-43.
5. Park S, Choi BW, Rim SJ, Shim CY, Ko YG, Kang SM, et al. Delayed hyperenhancement magnetic resonance imaging is useful in predicting functional recovery of nonischemic left ventricular systolic dysfunction. J Card Fail 2006;12:93-9.
6. Assomull RG, Prasad SK, Lyne J, Smith G, Burman ED, Khan M, et al. Cardiovascular magnetic resonance, fibrosis, and prognosis in dilated cardiomyopathy. J Am Coll Cardiol 2006;48:1977-85.
7. Bello D, Shah DJ, Farah GM, Di Luzio S, Parker M, Johnson MR, et al. Gadolinium cardiovascular magnetic resonance predicts reversible myocardial dysfunction and remodeling in patients with heart failure undergoing beta-blocker therapy. Circulation 2003;108:1945-53.
8. Swynghedauw B. Molecular mechanisms of myocardial remodeling. Physiol Rev 1999;79:215-62.
9. Saraste A, Nekolla SG, Schwaiger M. Cardiovascular molecular imaging: An overview. Cardiovasc Res 2009;83(4):643–52.
10. Shirani J, Narula J, Eckelman WC, Narula N, Dilsizian V. Early imaging in heart failure: Exploring novel molecular targets. J Nucl Cardiol 2007;14:100-10.
11. Dilsizian V, Eckelman WC, Loredo ML, Jagoda EM, Shirani J. Evidence for tissue angiotensin-converting enzyme in explanted hearts of ischemic cardiomyopathy using targeted radiotracer technique. J Nucl Med 2007;48:182-7.
12. Verjans JWH, Lovhaug D, Narula N, Petrov AD, Indrevoll B, Bjurgert E, et al. Noninvasive imaging of angiotensin receptors after myocardial infarction. JACC Cardiovasc Imaging 2008;1:354-62.
13. van den Borne SW, Isobe S, Verjans JW, Petrov A, Lovhaug D, Li P, et al. Molecular imaging of interstitial alterations in remodeling myocardium after myocardial infarction. J Am Coll Cardiol 2008;52:2017-28.
14. Haubner R, Weber WA, Beer AJ, Vabuliene E, Reim D, Sarbia M, et al. Noninvasive visualization of the activated alphavbeta3 integrin in cancer patients by positron emission tomography and [18F]Galacto-RGD. PLoS Med 2005;2:e70.
15. Bach-Gansmo T, Danielsson R, Saracco A, Wilczek B, Bogsrud TV, Fangberget A, et al. Integrin receptor imaging of breast cancer: A proof-of-concept study to evaluate 99mTc-NC100692. J Nucl Med 2006;47:1434-9.
16. van den Borne SW, Isobe S, Zandbergen HR, Li P, Petrov A, Wong ND, et al. Molecular imaging for efficacy of pharmacologic intervention in myocardial remodeling. JACC Cardiovasc Imaging 2009;2:187-98.
17. Schiller NB, Shah PM, Crawford M, DeMaria A, Devereux R, Feigenbaum H, et al. Recommendations for quantitation of the left ventricle by two-dimensional echocardiography. American Society of Echocardiography Committee on Standards, Subcommittee on Quantitation of Two-Dimensional Echocardiograms. J Am Soc Echocardiogr 1989;2:358-67.
18. Kietselaer BL, Reutelingsperger CP, Boersma HH, Heidendal GA, Liem IH, Crijns HJ, et al. Noninvasive detection of programmed cell loss with 99mTc-labeled annexin A5 in heart failure. J Nucl Med 2007;48:562-7.
19. Frangogiannis NG, Smith CW, Entman ML. The inflammatory response in myocardial infarction. Cardiovasc Res 2002;53:31-47.
20. Desmouliere A, Redard M, Darby I, Gabbiani G. Apoptosis mediates the decrease in cellularity during the transition between granulation tissue and scar. Am J Pathol 1995;146:56-66.
21. Sun M, Opavsky MA, Stewart DJ, Rabinovitch M, Dawood F, Wen WH, et al. Temporal response and localization of integrins beta1 and beta3 in the heart after myocardial infarction: Regulation by cytokines. Circulation 2003;107:1046-52.
22. Meoli DF, Sadeghi MM, Krassilnikova S, Bourke BN, Giordano FJ, Dione DP, et al. Noninvasive imaging of myocardial angiogenesis following experimental myocardial infarction. J Clin Invest 2004;113:1684-91.
23. Hua J, Dobrucki LW, Sadeghi MM, Zhang J, Bourke BN, Cavaliere P, et al. Noninvasive imaging of angiogenesis with a 99mTc-labeled peptide targeted at alphavbeta3 integrin after murine hindlimb ischemia. Circulation 2005;111:3255-60.
24. McMurray JJ, Ostergren J, Swedberg K, Granger CB, Held P, Michelson EL, et al. Effects of candesartan in patients with chronic heart failure and reduced left-ventricular systolic function taking angiotensin-converting-enzyme inhibitors: The CHARM-Added trial. Lancet 2003;362:767-71.
25. Cohn JN, Tognoni G. A randomized trial of the angiotensin-receptor blocker valsartan in chronic heart failure. N Engl J Med 2001;345:1667-75.